JOURNAL OF PROPULSION AND POWER
Vol. 22, No. 6, November–December 2006

Segmented Electrode Hall Thruster

Kevin D. Diamant,* James E. Pollard,† and Ronald B. Cohen‡
The Aerospace Corporation, Los Angeles, California 90009
and
Yevgeny Raitses§ and Nathaniel J. Fisch‖
Princeton University Plasma Physics Laboratory, Princeton, New Jersey 08543

DOI: 10.2514/1.19417

Thrust, thrust efficiency, and plume divergence were measured for a 9 cm diam laboratory model Hall thruster with segmented electrodes in the discharge channel. Several geometries with graphite nonemissive electrodes, and one with a tungsten emissive electrode were tested and compared to a baseline configuration with all electrodes replaced by boron nitride segments. To within measurement uncertainty, thrust and thrust efficiency were unaffected by insertion of electrodes, with the exception of reduced efficiency for a configuration which resulted in a 20% increase in discharge current. Maximum plume half-angle reductions of 4 deg were obtained with emissive and nonemissive electrodes.

Nomenclature

B	=	magnetic field
J_ϕ	=	plume ion current contained within half-angle ϕ
j	=	ion current density at plume probe
$\dot{m}$	=	anode xenon mass flow rate
P	=	discharge power
R	=	distance to plume probe
T	=	thrust
η_T	=	thrust efficiency
θ	=	angular location of plume probe
ϕ	=	plume half-angle

I. Introduction

THE relatively large plume divergence of Hall thrusters complicates spacecraft integration. Impingement of plasma on spacecraft surfaces can lead to functional degradation as well as thrust reduction and torques on the spacecraft. Hall thruster plume geometry is determined by the ion-accelerating electric field, which in turn is most strongly influenced by the applied magnetic field and the material properties of the discharge channel. This paper presents results from an effort to reduce plume divergence through insertion of electrodes in the discharge channel.

Fisch et al. [1] proposed the use of thermionic electron emitting (emissive) electrodes to impress potentials in the channel (also proposed by Morozov et al. [2]), with the goal of localizing most of the electric field in a region of concave magnetic field curvature, resulting in focusing of the ion beam. It was assumed that emissive electrodes would be required to provide sufficient current to reduce the sheath that would otherwise shield the electrode potential from the bulk plasma. A nominally 1 kW, 9 cm diam thruster was designed and built to test this idea (Fig. 1) [1]. A summary of major findings to date is as follows.

A LaB_6 coated electrode placed on the discharge channel inside diameter near the thruster exit plane resulted in plume half-angle reductions of up to 10 deg at some operating conditions [3]. This electrode did not have an integral heater, and electron emission was primarily due to ion collection. The largest reductions in plume divergence were observed with the electrode biased to cathode potential, but similar reductions were obtained with the electrode floating. Some degradation in thruster performance was measured, and it was noted that the channel became coated with metal sputtered from the electrode. The addition of a second floating electrode on the channel outside diameter at distances of 10 or 16 mm upstream of the inner electrode was found to improve performance while retaining nearly the same plume divergence reduction [4].

To reduce electrode sputtering, and because favorable results were obtained with nonemissive electrodes, a carbon–carbon-fiber electrode was tested on the channel inside diameter near the thruster exit [5]. Plume half-angle reductions of approximately 5 deg were measured with the electrode biased to cathode potential or floating. Plasma potential measurements in the channel indicated that the electrode caused the acceleration region to move a few millimeters upstream, and it was suggested that the reduced divergence resulted from a reduction in the voltage drop occurring outside the channel in a region of fringing (convex) magnetic field lines. A second floating carbon–carbon-fiber electrode placed on the channel outer diameter directly across from the inner electrode resulted in a plume half-angle reduction of 9 deg [6]. It was postulated that this second electrode simulated the effect of the conductive coating produced by sputtering of the LaB_6 electrode described in [3]. Modeling indicated that the presence of low secondary electron emission (SEE) material in the channel could have been responsible for shifting the acceleration region upstream and reducing the plume divergence [7]. Recent experimental results have demonstrated the effect of low SEE carbon electrodes on the electron temperature [8], in qualitative agreement with several thruster models [9–11]. Modeling by Fruchtman et al. suggests that an electrode in the channel may enhance efficiency and provide control of the electric field profile in the thruster [12].

Diamant et al. [13] describes our first attempt to obtain independent confirmation of the results presented in [1,3–6]. Nonemissive graphite electrodes were used, and electromagnet currents were held constant. Maximum plume half-angle reductions of approximately 2 deg were obtained for a few cases, whereas most resulted in increased divergence. Because the magnetic field geometry exerts a strong influence on the plume profile [6,14,15],

Presented as Paper 4098 at the 40th AIAA/ASME/SAE/ASEE Joint Propulsion Conference and Exhibit, Fort Lauderdale Florida, 11–14 July 2004; received 17 August 2005; revision received 15 February 2006; accepted for publication 17 February 2006.

*Senior Member of Technical Staff, Propulsion Science and Experimental Mechanics, M5-754. Member AIAA.
†Senior Scientist, Propulsion Science and Experimental Mechanics, M5-754. Member AIAA.
‡Director, Propulsion Science and Experimental Mechanics, M5-754. Member AIAA.
§Research Physicist. Member AIAA.
‖Director of Program in Plasma Physics and Professor of Astrophysical Sciences, MS30, C-Site, T162. Member AIAA.

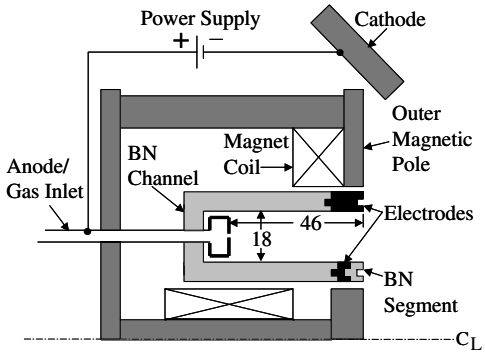

Fig. 1 Hall thruster cross section with segmented electrodes, dimensions in millimeters.

and because different channel configurations may require different optimum values of the magnetic field, in this study the magnetic field was adjusted for minimum plume divergence (except as noted in Sec. III.B) while testing several more electrode geometries similar to those investigated in [1,3–6].

II. Experiment

The Hall thruster was mounted in a 2.4-m diam × 9.8-m long vacuum chamber equipped with four reentrant cryopumps and three 4-ft diam cryotubs. At a xenon flow rate of 2.0 mg/s, the chamber pressure was approximately 2×10^{-6} torr (corrected for xenon). Xenon flow rates to the anode and cathode were regulated by thermal mass flow controllers.

The 9 cm thruster is described in [3]. Operating conditions were the following: anode flow rate of 1.7 mg/s, cathode flow rate of 0.30 mg/s, and discharge voltages of 200, 250, and 300 V. Discharge current without electrodes was typically 1.4 A. The boron nitride (BN) channel was modified to permit installation of electrodes, or BN segments in place of electrodes, with a tongue-in-groove design that allowed electrode surfaces to be flush with the channel. In keeping with the earlier nomenclature [1,3,4], the configuration shown in Fig. 1 will be referred to as TS1 when the outer electrode was floating and TS1B when the outer electrode was biased to cathode potential. In that configuration the most downstream edge of the inner electrode was 2 mm upstream of the channel exit. Three other electrode configurations with no outer electrode will be referred to as NS1, NS2, and NS3, for cases in which the downstream edge of the inner electrode was at the channel exit, or 2, or 4 mm upstream of the channel exit, respectively. The various configurations are diagrammed in Fig. 2, including the "baseline" configuration for which electrodes were replaced by BN segments. Electrodes were graphite, except for one experiment with an emissive electrode in configuration NS1. Electrodes placed on the channel inside diameter were 4 mm wide, whereas the electrode placed on the outside diameter was 10 mm wide.

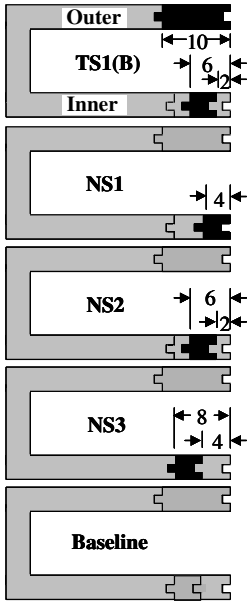

Fig. 2 Channel cross sections showing electrode configurations, dimensions in millimeters. Black = electrode, gray = BN.

The emissive electrode is described in [14] and is a tungsten dispenser ring cathode with an integral filament heater. Substantial electron emission was achieved at a surface temperature of approximately 1100°C, with a heater power of 300 W. Surface temperature was measured with a vanishing filament optical pyrometer with a measurement uncertainty of about 20°C.

Plume ion flux was recorded with a retarding potential analyzer (RPA) described in [16]. RPA scans were recorded at a radius of 1 m from the thruster exit plane in 2.5 deg angular steps with retarding potentials of 0, 25, and 50 V with respect to ground. Thruster electromagnet current settings for minimum plume divergence were determined by minimizing the RPA signal with a 0 V repelling bias at 60 deg from the thruster centerline. This procedure also resulted in minimization of the discharge current (Sec. 3.2 of [17] describes how a magnetic field properly configured for discharge current minimization will result in favorable ion focusing).

The thruster was mounted on an inverted pendulum thrust stand, described in [18]. Thrust was measured with a strain gauge gram sensor. A second gram sensor was attached to the thruster mounting bracket for stand calibration. A continuously variable load could be applied to the calibration sensor by a stepper motor drawing up a fishing line attached to the sensor through a spring. Calibration was performed after every thrust reading. Thrust measurement resolution was 0.1 mN with an accuracy of approximately 1 mN.

III. Results and Discussion

A. Data Reduction

Hall thruster performance was evaluated through the experimental determination of T, η_T, and plume divergence. Thrust efficiency was determined as the ratio of directed thrust power to P:

$$\eta_T = T^2/(2\dot{m}P) \tag{1}$$

Measurement uncertainty for thrust efficiency was approximately 10% (e.g., 30 ± 3%). Assuming an azimuthally symmetric plume, the current J_ϕ contained within ϕ is given by

$$J_\phi = 2\pi R^2 \int_0^\phi j \sin\theta \mathrm{d}\theta \tag{2}$$

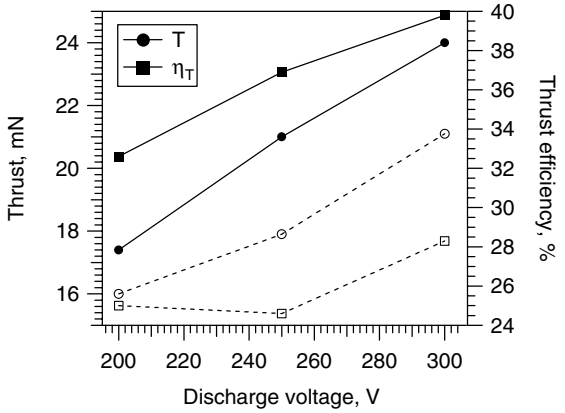

Fig. 3 Baseline thrust (±1 mN) and efficiency (±10%). Closed symbols: *B* set for minimum plume divergence; open symbols: *B* set for maximum divergence without unstable operation.

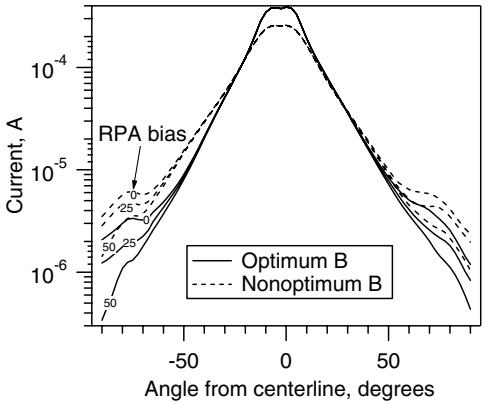

Fig. 4 Baseline plume profiles with optimum (minimum plume divergence) *B* and nonoptimum *B* at 300 V.

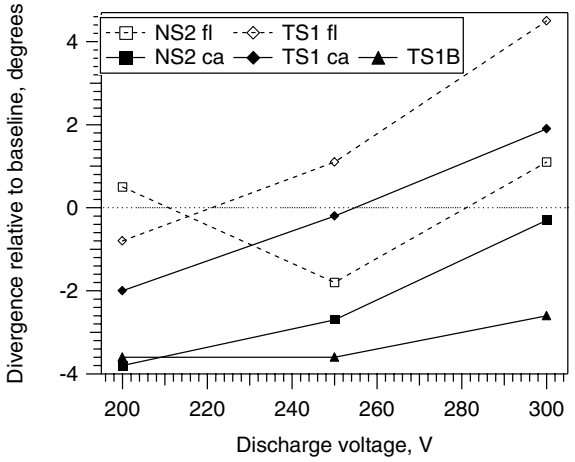

Fig. 5 Divergence (±1 deg) relative to baseline.

The radial distance R from the thruster exit plane to the RPA was 1 m. Plume divergence was calculated as the half-angle ϕ such that $J_\phi/J_{90\ \mathrm{deg}} = 0.95$. Typically, divergence measurements were repeatable to within less than 0.3 deg for scans recorded in immediate succession, however, the absolute uncertainty was set by the angle subtended by the RPA inlet aperture at 1 m, which was approximately 1 deg.

The thruster discharge channel typically became coated with sputtered electrode material. In an effort to obtain unambiguous results, sputtered material was removed from BN surfaces with light sandpaper between runs, and run times were limited to approximately 3 h. With these precautions, on average the differences in thrust and discharge current between the same operating point at the beginning and end of a run were within the uncertainty of the measurements (discharge current uncertainty was about 1%). Differences in divergence were ±1.6 deg on average.

B. Baseline Performance and Effect of Magnetic Field

The effect of B on thrust and thrust efficiency in the baseline configuration is shown in Fig. 3. Data are shown for B adjusted for minimum plume divergence (optimum), and for B adjusted for maximum plume divergence (nonoptimum) without causing unstable operation or excessive discharge current. Beam profiles recorded at a discharge voltage of 300 V in the baseline configuration with both optimum and nonoptimum B are shown in Fig. 4. The increase in plume divergence, averaged over the three RPA biases and the three discharge voltages, for nonoptimum B relative to optimum B for the baseline channel configuration was 8 deg. For the remainder of the data presented here, B was adjusted for minimum divergence.

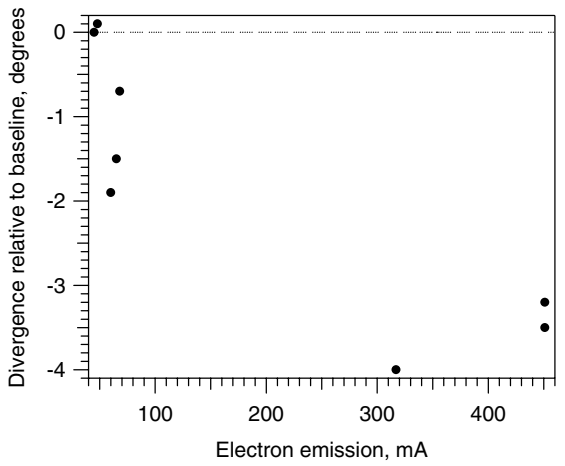

Fig. 6 Divergence (±1 deg) relative to baseline vs electron emission for emissive electrode at NS1 (250 V).

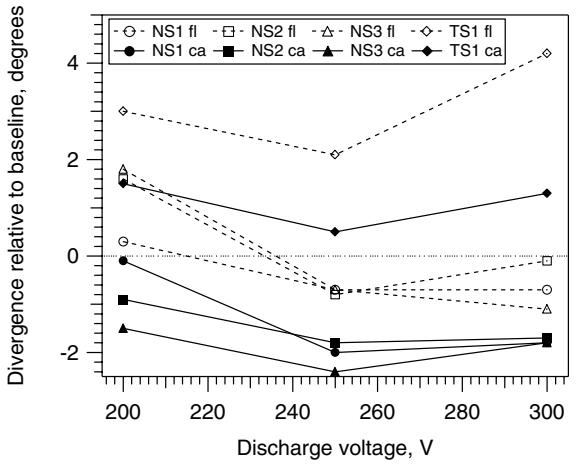

Fig. 7 Divergence (±1 deg) relative to baseline with BN coat on outer magnetic pole.

C. Divergence with Electrodes

Figures 5–8 show differences in plume divergence relative to the baseline configuration for graphite (nonemissive) electrodes. Because it was found that they were not strongly affected by RPA bias, all relative divergence measurements are averages over the three RPA biases. Negative values indicate reduced divergence relative to the baseline. For the NS cases the electrode was either allowed to float (fl) or was biased to cathode potential (ca). For TS1 the outer electrode was floating while the inner was either floating or cathode biased. Both electrodes were cathode biased in case TS1B. Cathode potential was typically between 16 and 17 V below ground. Floating potentials relative to ground for the various electrode positions are shown in Fig. 9.

Figure 5 displays results for NS2, TS1, and TS1B. The NS2 results at 200 and 250 V approach the 5 deg half-angle reduction reported in [6] for 250 V. However, the TS1 results differ considerably from the 9 deg half-angle reduction reported in [6]. It is interesting to note that the floating potential at the position of the NS2 electrode (TS1 inner) increases with the addition of the outer floating electrode. This may indicate a downstream migration of the acceleration region, with resulting increase in plume divergence (see also Fig. 7) as discussed in [5]. For both NS2 and TS1 the best results were obtained with cathode bias, and motivated investigation of case TS1B. The large outer electrode increased the net electrode ion collection from an average of about 60 mA to approximately 200 mA and resulted in the most consistent reductions in plume divergence.

Figure 6 shows the results obtained with a cathode biased emissive electrode in configuration NS1 at a discharge voltage of 250 V. Data

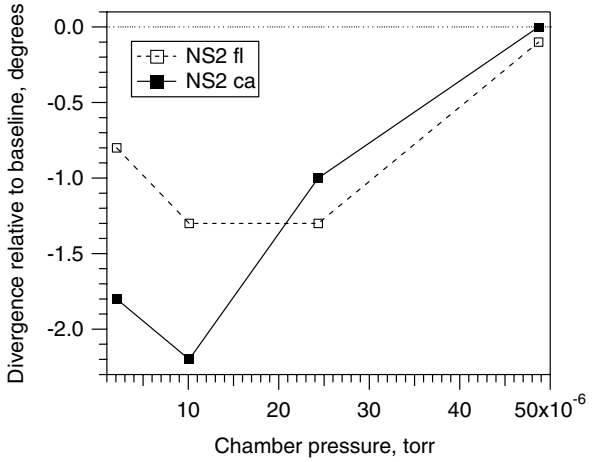

Fig. 8 Divergence (±1 deg) at elevated pressure and 250 V discharge voltage with BN coat on outer magnetic pole.

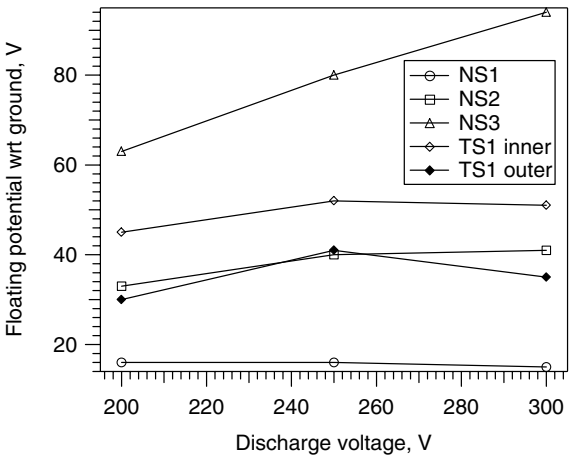

Fig. 9 Electrode floating potentials (±1 V).

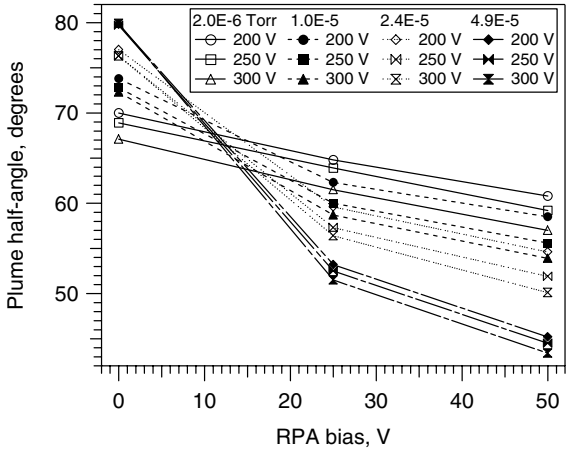

Fig. 10 Baseline divergence (±1 deg) as a function of chamber background pressure at 250 V.

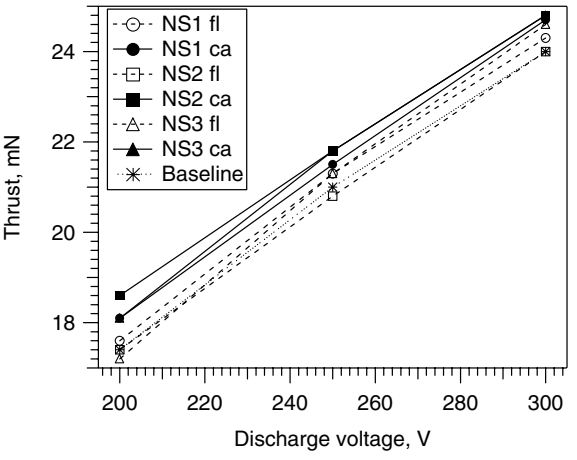

Fig. 11 Thrust (±1 mN) for configurations NS1, NS2, NS3, and the baseline.

at values of electron emission below 100 mA were obtained with no heater power (electron emission by ion collection). With about 300 W of heater power, emission was raised to 320 and 450 mA, at which points the divergence reduction was close to that obtained for cases NS2 and TS1B. The divergence reduction was also nearly the same as that reported in [3] for the LaB_6 electrode at position NS1 with cathode bias (about 5 deg).

To eliminate the possibility that material sputtered from the exposed outer magnetic pole (low carbon steel) was entering the discharge channel and influencing plume divergence, the outer pole was coated with BN. This coating was not present in [1,3–6]. Figure 7 shows that for cases NS1, NS2, NS3, and TS1 the largest plume divergence reduction with the BN coating was only 2 deg.

The typical background pressure reported in [1,3–6] was 2×10^{-5} torr. Through a combination of running fewer pumps and bleeding in excess xenon through a port near the thruster, configuration NS2 was tested at pressures from 1×10^{-5} to 5×10^{-5} torr at a discharge voltage of 250 V. The BN coating was present on the outer magnetic pole for these tests. The results (relative to baseline measurements recorded at the same elevated pressures) shown in Fig. 8 are not better than those obtained at 2×10^{-6} torr. While performing this experiment, the data shown in Fig. 10 were obtained for the baseline configuration. These data, reported here as a matter of general interest, show that facility background pressure can lead to erroneously large values of plume divergence if low energy charge exchange ions are not screened out (0 RPA bias), or to erroneously small values if they are. This latter effect is presumably due to the larger probability of charge exchange reactions involving the lower energy ions that populate the plume at large angles [19].

D. Performance with Electrodes

Figures 11 and 12 show thrust for all of the configurations tested, and in general the differences between configurations were within the thrust stand measurement uncertainty (1 mN). Thrust with the emissive electrode did not vary significantly with the level of emission, and so the data point shown in Fig. 12 (overlays baseline at 250 V) is an average over all measurements taken.

Figures 13 and 14 present thrust efficiencies. The cathode biased efficiencies shown in Fig. 13 suffered from a 3% on average increase in the discharge current relative to the baseline (floating cases increased by less than 1% relative to the baseline). A 3% increase is consistent with the roughly 60 mA (out of 1.4 A of discharge current for the baseline configuration) of ion current collected by the cathode biased electrode. The cases shown in Fig. 14 all suffered from much larger increases in the discharge current. Regardless of bias on the inner electrode, TS1 resulted in an 11% on average increase in discharge current. Perhaps the outer floating electrode provided a conductor through which electrons could travel upstream outside of the plasma [14,20]. For TS1B the increase in discharge current was nearly 20%, presumably due to a combination of short-circuiting the magnetic field (as in TS1) and the larger area available for ion collection. The increase in discharge current for the emissive electrode was not strongly dependent on the level of emission and was about 8% on average. The power required to heat the emissive electrode was responsible for the large reduction in efficiency.

Total plume ion current ($J_{90\ \mathrm{deg}}$ at 0 V RPA bias), and therefore electron current to the plume, was found to be nearly unaffected by the presence of electrodes in the channel. On average, for all operating points, the difference between the various electrode configurations and the baseline was 1%. Therefore we may conclude

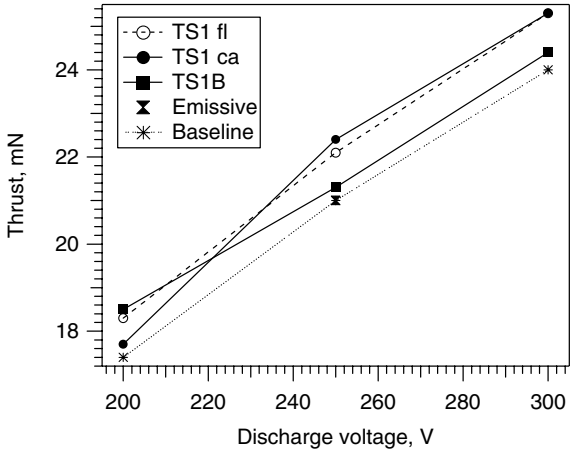

Fig. 12 Thrust (±1 mN) for configurations TS1, TS1B, emissive electrode at NS1, and the baseline.

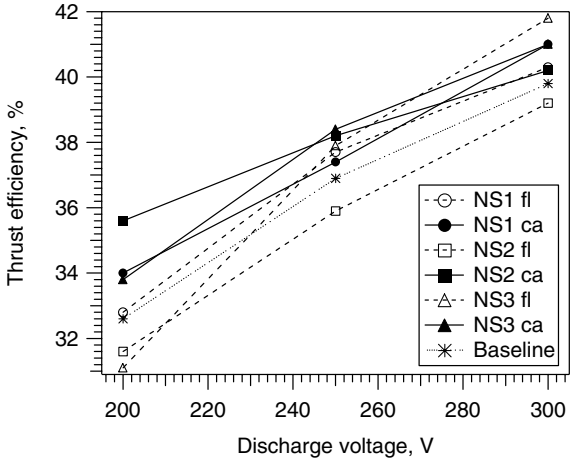

Fig. 13 Thrust efficiency (±10%) for configurations NS1, NS2, NS3, and the baseline.

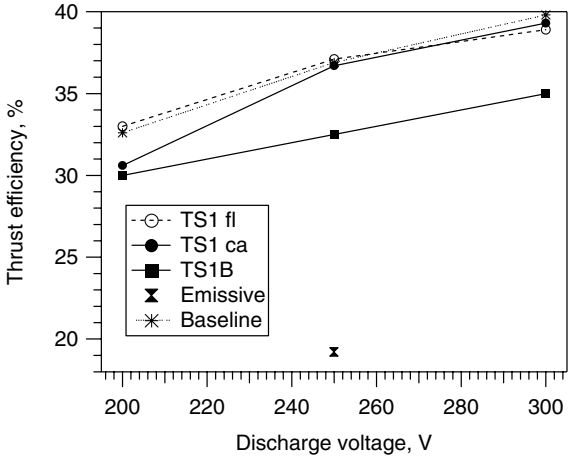

Fig. 14 Thrust efficiency (±10%) for configurations TS1, TS1B, emissive electrode at NS1, and the baseline.

that for NS cases with nonemissive electrodes, the amount of electron current entering the channel from the external cathode was nearly unchanged, because the discharge current either remained unchanged with electrodes floating, or increased by very nearly the value of the ion current collected with cathode bias. For TS cases, the amount of current entering the channel from the external cathode increased. In contrast, the discharge current increase with the emissive electrode was approximately 110 mA, whereas the total electron emission was 320–450 mA. If we assume that electrons leaving the emissive electrode were all collected at the anode, then the amount of electron current entering the channel from the external cathode must have decreased by 210–340 mA (a similar result was reported in [14]). These values represent 15 to 25% of the discharge current, which is approximately the amount the external cathode supplies to the discharge channel in a typical Hall thruster. It is interesting then that the emissive electrode, which appeared to substantially reduce the amount of electron current traversing the fringing magnetic fields between the external cathode and discharge channel, did not outperform the nonemissive electrodes with regard to divergence reduction. Perhaps divergence reduction is more closely related to the material properties of the electrodes, or perhaps bypassing the fringing fields outside the thruster is of limited benefit.

IV. Conclusion

A 9 cm laboratory model Hall thruster was tested with a discharge channel modified to allow the insertion of segmented electrodes. Earlier testing had demonstrated that for some operating conditions electrodes in the channel could substantially reduce plume divergence. In this work we examined several electrode geometries closely matching those used in [1,3–6]. Plume half-angle reductions of nearly 4 deg for a single emissive or nonemissive electrode on the channel inside diameter near the exit were roughly in agreement with 5 deg reductions observed in [5]. However, a second floating electrode placed on the channel outer diameter at the exit resulted in at most a 2 deg divergence reduction, while a 9 deg reduction was reported in [6]. When that outer electrode was biased to the cathode potential, divergence reduction comparable to the emissive electrode was obtained. The mechanism for divergence reduction is not fully understood, nor do we understand why in some cases our results do not agree with those reported in [1,3–6]. A remaining difference between this work and those references is that our plume scans were recorded at a radius of 1 m, rather than at 33 cm. Also, the ion flux probe used in [1,3–6] was a guarded, negatively biased flat plate, whereas we used an RPA. Additional testing would be required to determine the significance of these differences.

Acknowledgment

This work was supported under The Aerospace Corporation's Mission Oriented Investigation and Experimentation program, funded by the U.S. Air Force Space and Missile Systems Center under Contract No. FA8802-04-C-0001.

References

[1] Fisch, N. J., Raitses, Y., Litvak, A., and Dorf, L., "Design and Operation of Hall Thruster with Segmented Electrodes," AIAA Paper 99-2572, June 1999.

[2] Morozov, A.I., Esinchuk, Y.V., Tilinin, G.N., Trofimov, A.V., Sharov, Y.A., and Shchepkin, G.Y., "Plasma Accelerator with Closed Electron Drift and Extended Acceleration Zone," *Soviet Physics Technical Physics*, Vol. 17, No. 1, July 1972, pp. 38–45.

[3] Raitses, Y., Dorf, L. A., Litvak, A. A., and Fisch, N. J., "Plume Reduction in Segmented Electrode Hall Thruster," *Journal of Applied Physics*, Vol. 88, No. 3, Aug. 2000, pp. 1263–1270.

[4] Fisch, N. J., Raitses, Y., Dorf, L. A., and Litvak, A. A., "Variable Operation of Hall Thruster with Multiple Segmented Electrodes," *Journal of Applied Physics*, Vol. 89, No. 4, Feb. 2001, pp. 2040– 2046.

[5] Raitses, Y., Staack, D., Smirnov, A., Litvak, A. A., Dorf, L. A., Graves, T., and Fisch, N. J., "Studies of Non-Conventional Configuration Closed Electron Drift Thrusters," AIAA Paper 2001-3776, July 2001.

[6] Raitses, Y., Staack, D., and Fisch, N. J., "Measurements of Plasma Potential Distribution in Segmented Electrode Hall Thruster," IEPC Paper 01-060, Oct. 2001.

[7] Raitses, Y., Keidar, M., Staack, D., and Fisch, N. J., "Effects of Segmented Electrode in Hall Current Plasma Thrusters," *Journal of Applied Physics*, Vol. 92, No. 9, Nov. 2002, pp. 4906–4911.

[8] Raitses, Y., Smirnov, A., Staack, D., and Fisch, N.J., "Measurements of Secondary Electron Emission Effects in the Hall Thruster Discharge," *Physics of Plasmas*, Vol. 13, Jan. 2006, pp. 1–4.
[9] Barral, S., Makowski, K., Peradzynski, Z., Gascon, N., and Dudeck, M., "Wall Material Effects in Stationary Plasma Thrusters II. Near-Wall and In-Wall Conductivity," *Physics of Plasmas*, Vol. 10, No. 10, Oct. 2003, pp. 4137–4152.
[10] Keidar, M., Boyd, I. D., and Beilis, I. I., "Plasma Flow and Plasma-Wall Transition in Hall Thruster Channel," *Physics of Plasmas*, Vol. 8, No. 12, Dec. 2001, pp. 5315–5322.
[11] Ahedo, E., and Escobar, D., "Influence of Design and Operation Parameters on Hall Thruster Performances," *Journal of Applied Physics*, Vol. 96, No. 2, July 2004, pp. 983–992.
[12] Fruchtman, A., Fisch, N.J., and Raitses, Y., "Control of the Electric-Field Profile in the Hall Thruster," *Physics of Plasmas*, Vol. 8, No. 3, March 2001, pp. 1048–1056.
[13] Diamant, K. D., Pollard, J. E., Cohen, R. B., Raitses, Y., and Fisch, N. J., "Plume Characteristics of the PPPL Segmented Electrode Hall Thruster," AIAA Paper 2003-5159, July 2003.
[14] Raitses, Y., Staack, D., and Fisch, N. J., "Plasma Characterization of Hall Thruster with Active and Passive Segmented Electrodes," AIAA Paper 2002-3954, July 2002.
[15] Gavryushin, V. M., and Kim, V., "Effect of the Characteristics of a Magnetic Field on the Parameters of an Ion Current at the Output of an Accelerator with Closed Electron Drift," *Soviet Physics Technical Physics*, Vol. 26, No. 4, April 1981, pp. 505–507.
[16] Pollard, J. E., and Diamant, K. D., "Hall Thruster Plume Shield Wake Structure," AIAA Paper 2003-5018, July 2003.
[17] Zhurin, V. V., Kaufman, H. R., and Robinson, R. S., "Physics of Closed Drift Thrusters," *Plasma Sources, Science and Technology*, Vol. 8, 1999, pp. R1–R20.
[18] Diamant, K. D., Brandenburg, J. E., Cohen, R. B., and Kline, J. F., "Performance Measurements of a Water Fed Microwave Electro-thermal Thruster," AIAA Paper 2001-3900, July 2001.
[19] Pullins, S., Dressler, R. A., Chiu, Y. H., and Levandier, D. J., "Ion Dynamics in Hall Effect and Ion Thrusters: $Xe + +Xe$ Symmetric Charge Transfer," AIAA Paper 2000-0603, Jan. 2000.
[20] Staack, D., Raitses, Y., and Fisch, N. J., "Control of the Acceleration Region in Hall Thrusters," IEPC 03-273, Toulouse, 2003.

R. Myers
Associate Editor